

*Supplementary information for*

**Anaerobic vs. Aerobic Preparation of Silicon Nanoparticles by Stirred Media Milling.  
The Effects of Dioxygen, Milling Solvent, and Milling Time on Particle Size,  
Surface Area, Crystallinity, Surface/Near-Surface Composition, and Reactivity**

Eric V. Bukovsky, Karlee P. Castro, Brent M. Wyatt,  
Olga V. Boltalina, and Steven H. Strauss

**Table of Contents**

<b>Fig. S-1.</b> Schematic drawing of the Netzsch MiniCer stirred-media attritor mill assembly	S-2
<b>Fig. S-2.</b> Photographs of Netzsch MiniCer mill and related equipment in the glovebox	S-3
<b>Table S-1.</b> Literature XPS peak positions	S-4
<b>Fig. S-3.</b> Typical BET plots for the determination of SiNP surface areas	S-5
<b>Fig. S-4.</b> PXRD pattern for a Si standard sample.	S-6
<b>Fig. S-5.</b> XPS Spectra of anaerobically heptane-milled SiNPs H-1, H-3, and H-5	S-7
<b>Fig. S-5.</b> TEM image of a single SiNP of HM(air)-5.5	S-8
<b>Fig. S-6.</b> TEM images of HM(air)-5.5 at two orthogonal beam orientations.	S-9
<b>Fig. S-7.</b> ATR-FTIR spectra of liquid heptane and mesitylene and solid pyrene	S-10
<b>Fig. S-8.</b> Tensimetric plots of $P(O_2)$ vs. time for HM-5 and MP-5 SiNPs	S-11
<b>Fig. S-9.</b> Anaerobic vs. aerobic BET surface areas for H, HM, and MP milled SiNPs	S-12
<b>References</b>	S-13

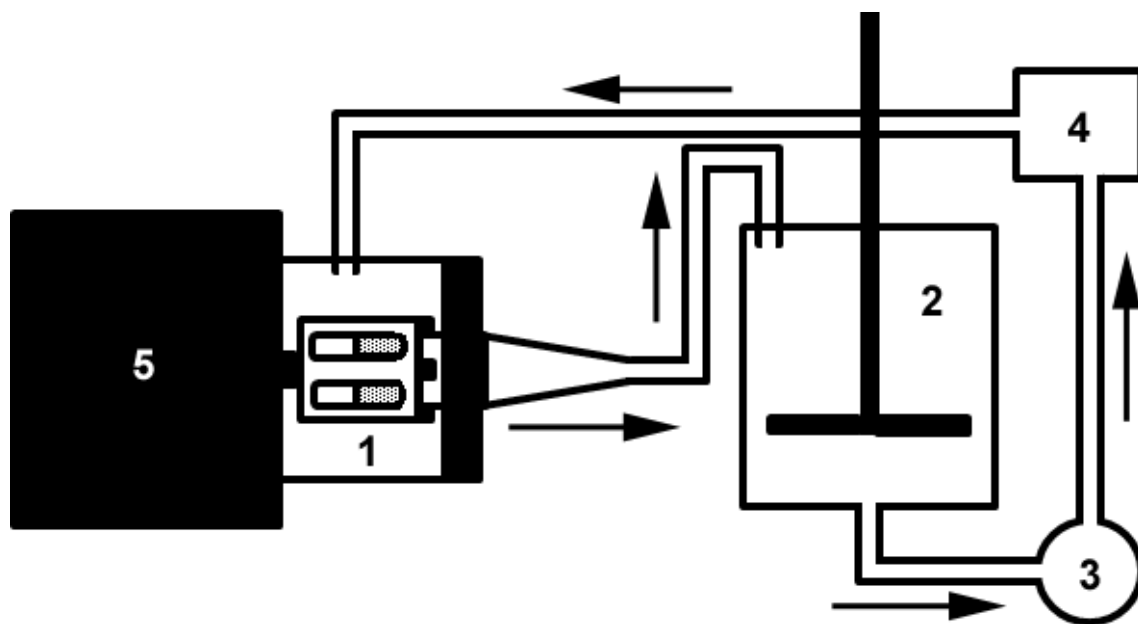


**Fig. S-1.** Schematic drawing of the Netzsch MiniCer stirred-media attritor mill and related equipment for the preparation of SiNPs. All of the tubing shown was either stainless steel or 1/8 in. I.D. Viton. (1) Water-cooled 160 mL milling chamber with double mechanical pressurized fluid seal, slotted cylinder mixer blade, and 150  $\mu\text{m}$  separator screen. (2) Stainless-steel 200 mL slurry mixing tank with overhead stirrer. (3) Peristaltic pump with 1/8 in. I.D. Viton tubing. (4) Sonicator with 1/2 in. diameter probe and low-flow cell. (5) Attritor mill motor. Not shown are the seal fluid tank, the rotary evaporator, cooling water lines, the power supply, control panel, and various electronics including interlocks to shut off the mill if the sonicator, peristaltic pump, or overhead stirrer lost power. Not shown are the valve and drain at the bottom of the mixing tank through which SiNP slurries were collected after a specified number of hours of milling.

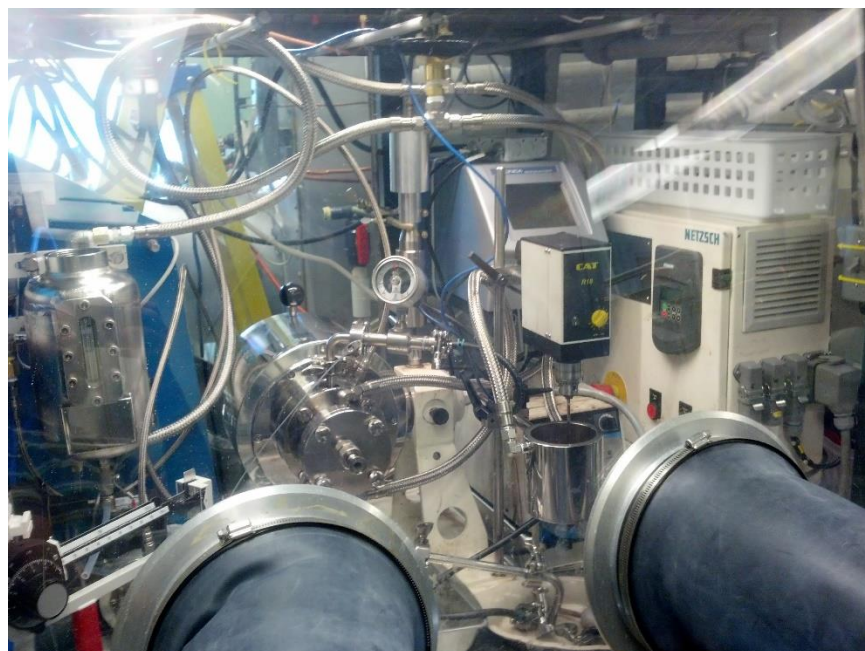


**Fig. S-2.** Photographs of Netzsch MiniCer attritor mill and related equipment (top) and the Buchi R11 rotary evaporator (bottom) side-by-side in the Vacuum Atmospheres HE-453-4 glovebox in the Strauss-Boltalina laboratory in the Department of Chemistry at Colorado State University.

**Table S-1.** Literature XPS peak positions relevant to this work

binding environment <sup>a</sup>	Si 2p peak positions, eV	carbon 1s peak positions, eV	oxygen 1s peak positions, eV
Si(0) 2p <sub>3/2</sub>	99.3, <sup>1-3</sup> 99.4, <sup>4</sup> 99.5 <sup>5-8</sup>	—	—
Si-C	99.9, <sup>9</sup> 100.0–100.4, <sup>10</sup> 100.3, <sup>3</sup> 101.0 <sup>11, 12</sup>	282.2, <sup>10</sup> 282.8, <sup>11</sup> 283.4, <sup>11</sup> 283.0, <sup>3</sup> 283.2 <sup>12</sup>	—
Si(II)	101.1, 101.7 (SiO), 101.5 (Si–Si <sub>2</sub> O <sub>3</sub> )	—	531.8 (Si–Si <sub>2</sub> O <sub>3</sub> ) <sup>5</sup>
Si(III)	102.1, <sup>1</sup> 102.1 (Si–Si <sub>2</sub> O <sub>3</sub> ), <sup>5</sup> 102.5 (Si–SiO <sub>3</sub> ) <sup>5</sup>	—	
Si(IV) (SiO <sub>2</sub> )	102.6, <sup>9</sup> 103.0, <sup>2</sup> 103.2, <sup>1, 4</sup> 103.3, <sup>3</sup> 103.4, <sup>12</sup> 103.5, <sup>5</sup> 103.8 <sup>6</sup>	—	532.4, <sup>4</sup> 532.5 <sup>1, 5, 6</sup>

<sup>a</sup> Silicon formal oxidation state are shown in parentheses. The literature cited in this Table are listed on the last page of this document and are not the same as the references with the same numbers in the primary paper for which this document is supplementary information.

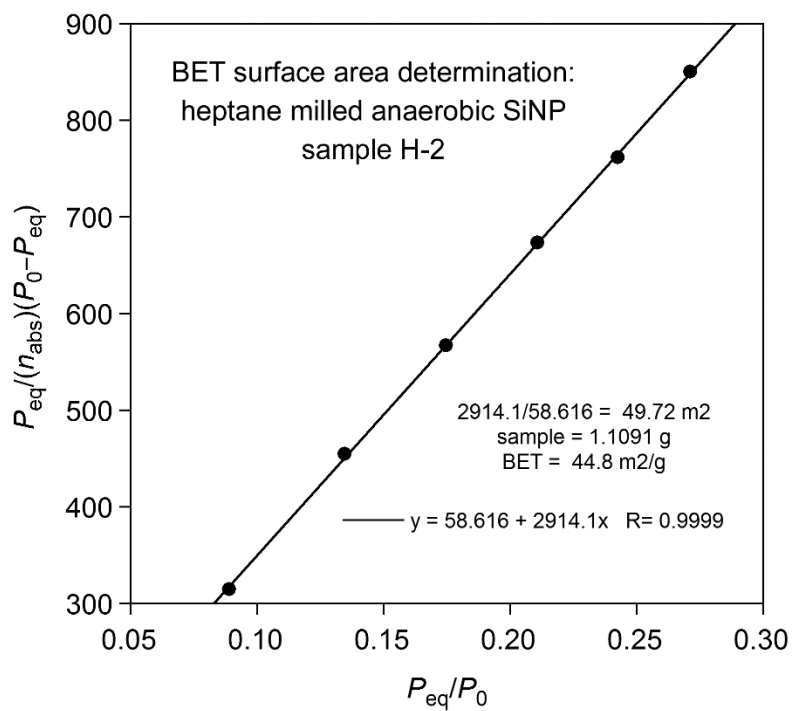
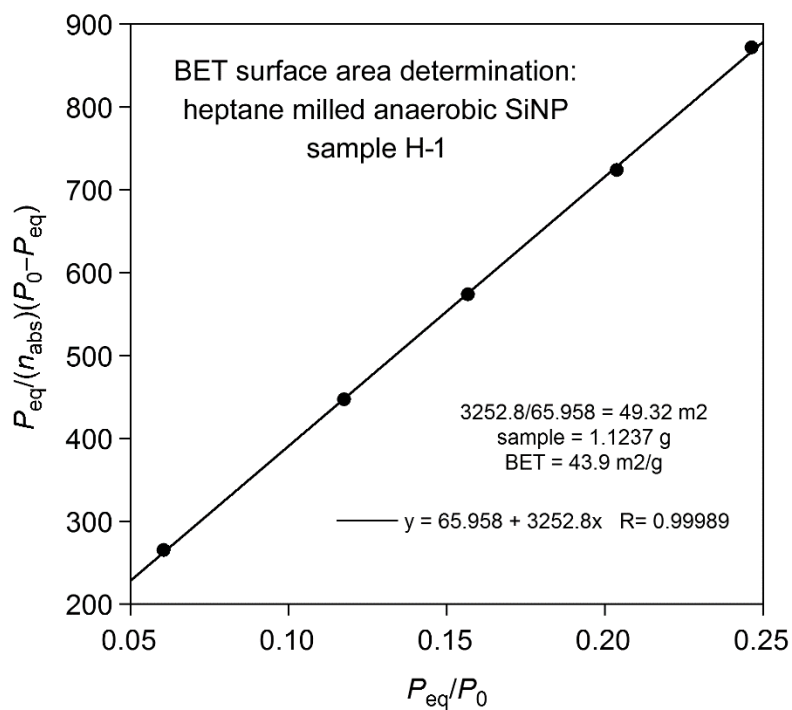


**Fig. S-3.** Typical BET plots for the determination of SiNP surface areas.

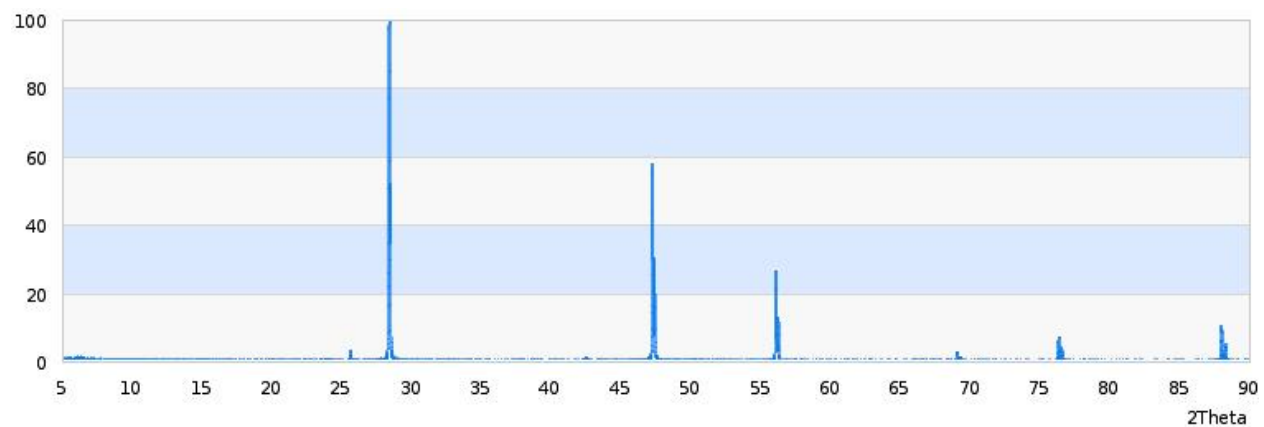


**Fig. S-4.** PXRD pattern for a Si standard sample (source: <http://www.mindat.org/min-3659.html>). Compare this pattern to the 0 h milling time PXRD pattern in Fig. 5.

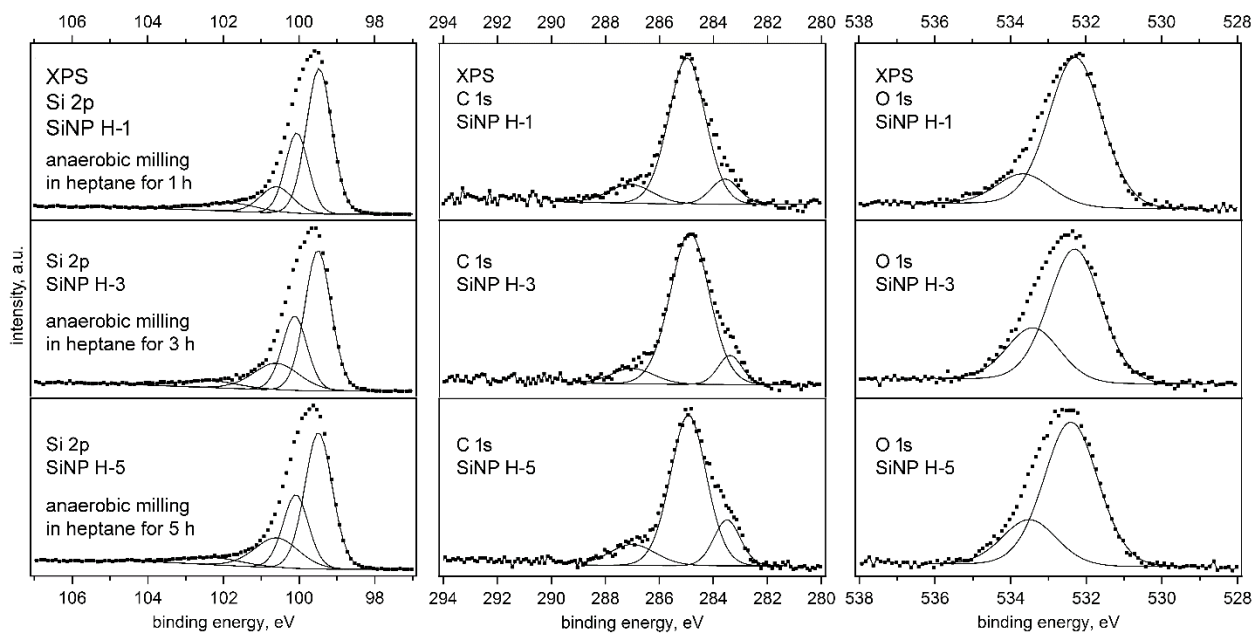


**Fig. S-5.** XPS Spectra of anaerobically heptane-milled SiNPs H-1, H-3, and H-5. The spectra indicate very little change in the surface/near-surface composition with respect to Si, C, and O after the first hour of milling.

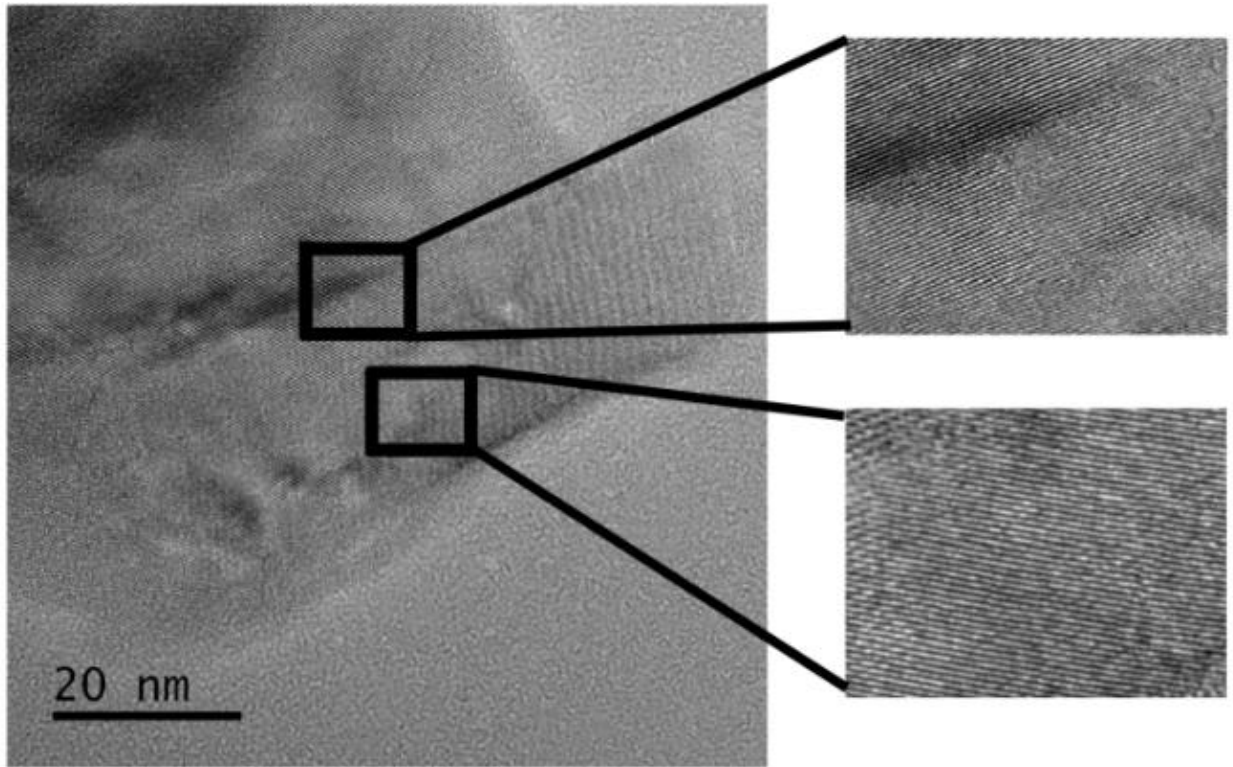


**Fig. S-6.** TEM image of a single SiNP of HM(air)-5.5 and expansions of two regions. Each expanded region appears to be a mozaic of crystallites with different orientations that are welded together. There are regions in the main image that appear to be amorphous.

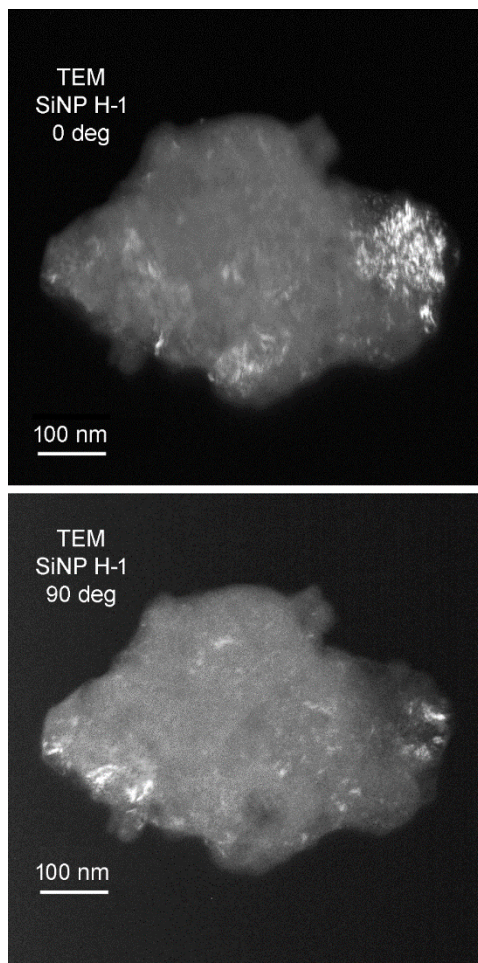


**Fig. S-7.** TEM images of HM(air)-5 at two orthogonal beam orientations.

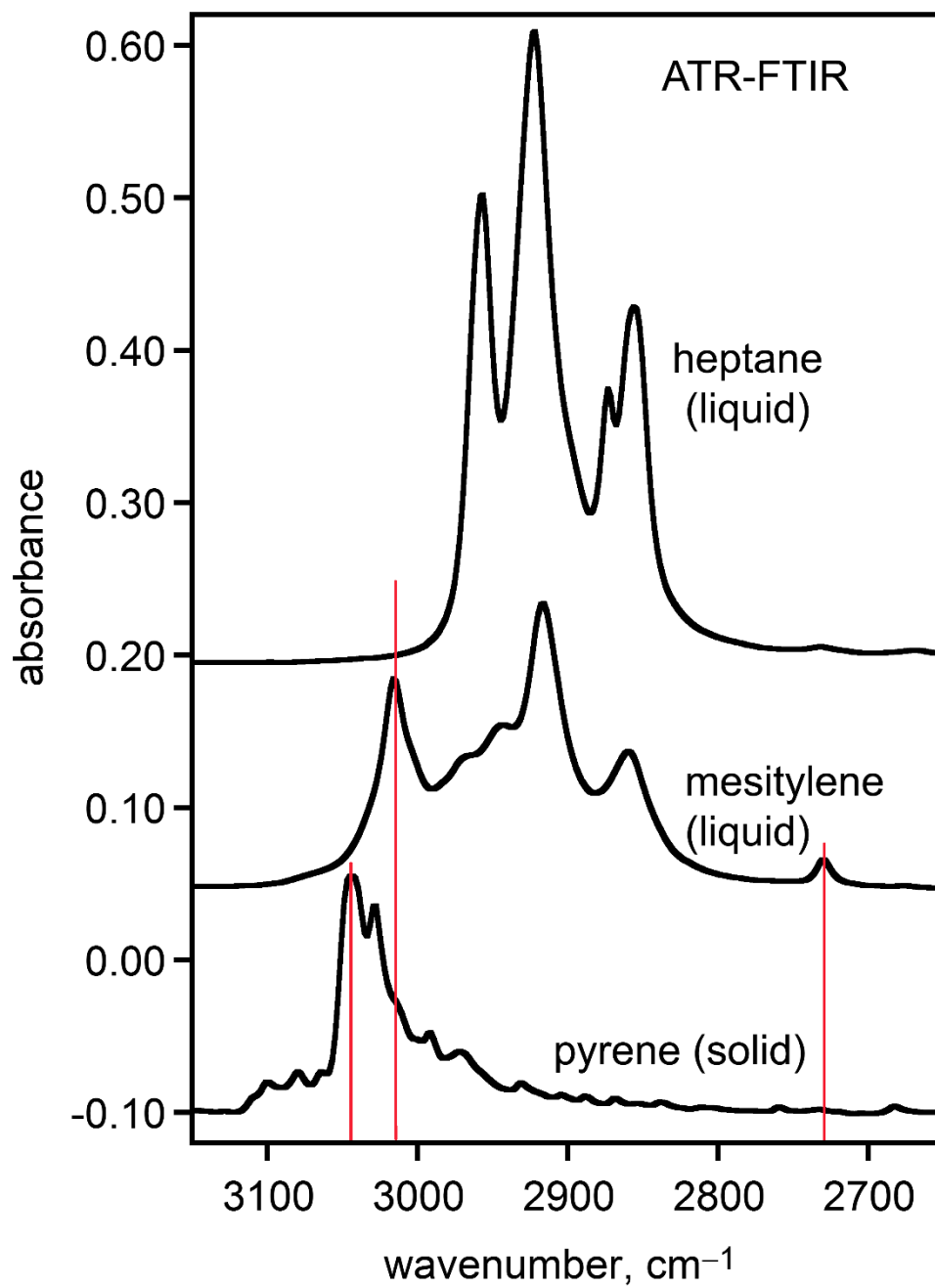


**Fig. S-8.** ATR-FTIR spectra of liquid heptane and mesitylene and solid pyrene.

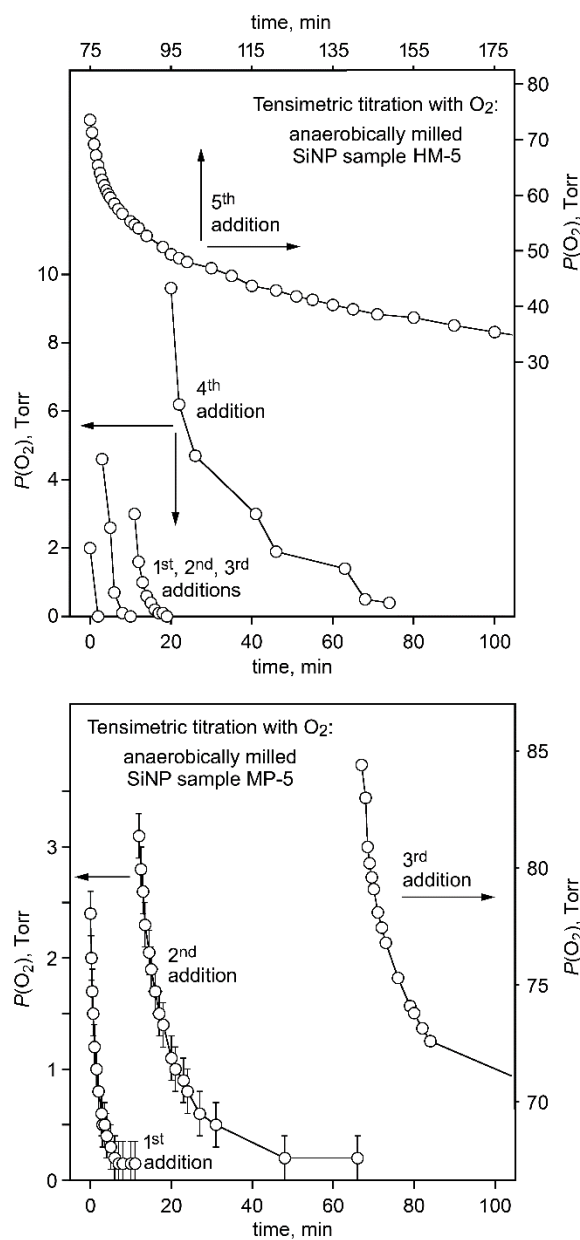


**Fig. S-9.** Plots of  $P(\text{O}_2)$  vs. time for anaerobically-milled SiNP samples of HM-5 and MP-5 exposed to several small measured doses of dioxygen gas. For HM-5 the initial pressures of eight sequential doses of dioxygen were 2.0, 4.6, 3.0, 9.6, 73.6, 83.1, 141.6, and 142.7 Torr (only the first five plots are shown). For MP-5 the initial pressures of five sequential doses of dioxygen were 2.4, 3.1, 84.4, and 73.6 Torr (only the first, second, and third plots are shown). The total amounts of dioxygen irreversibly absorbed by the samples were 1.6 mmol O<sub>2</sub>/g HM-5 and 1.2 mmol O<sub>2</sub>/g MP-5.

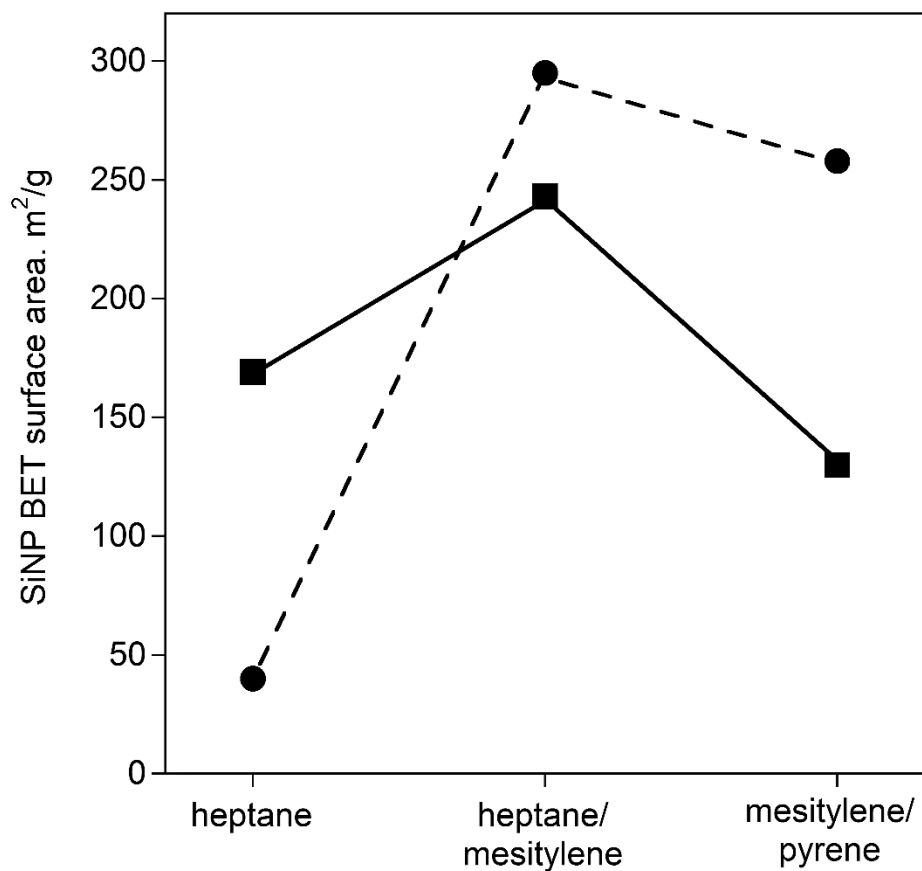
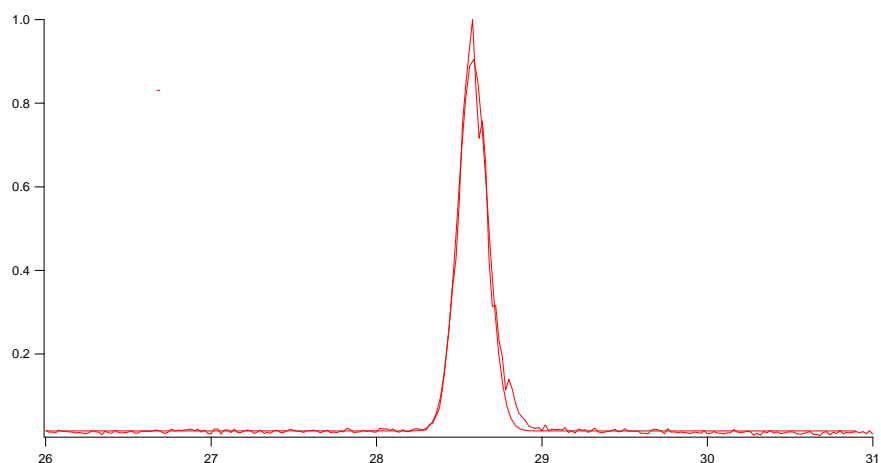


**Fig. S-10.** Anaerobic (circles) vs. aerobic (squares) BET surface areas for heptane, heptane/mesitylene, and mesitylene/pyrene milled SiNPs. The milling time was 5 h for the heptane and mesitylene/pyrene milled samples and 5.5 h for the heptane/mesitylene milled samples.

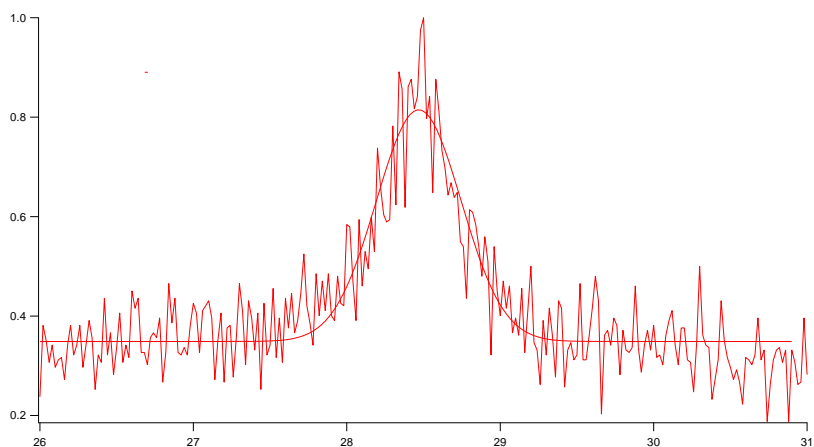
### Calculation of average crystallite size from PXRD patterns

Average crystallite sizes for samples MP-y ( $y = 1, 2, 5, 6$ ) and H-y ( $y = 1-5$ ) were determined using the Scherrer equation,  $T = (0.9)\lambda/\beta \cos(\theta)$ , to analyze the most intense peak in their PXRD patterns shown in Figure 5 in the main text ( $T$  is the mean size of ordered crystalline domains ("average crystallite size"),  $\lambda$  is the X-ray wavelength used (0.154 nm),  $\beta$  is the full-width at half maximum peak height (FWHM) in radians adjusted for intrinsic instrument broadening, and  $\theta$  is the Bragg angle).<sup>13,14</sup>

The most intense peak in each PXRD pattern was used ( $2\theta = 28.8 \pm 0.2^\circ$ ). Each was fit to a Gaussian curve, from which the FWHM was extracted. Two examples are shown below. The results are listed in Table 2 in the main text.



PXRD  $2\theta = 28.8^\circ$  peak for hand-ground 20–45  $\mu\text{m}$  particles of MGS Si fit to a Gaussian curve.



PXRD  $2\theta = 28.6^\circ$  peak for MP-2 SiNPs fit to a Gaussian curve.

## References for the Electronic supplementary information (i.e., this document)

1. A. M. Chockla, J. T. Harris, V. A. Akhavan, T. D. Bogart, V. C. Holmberg, C. Steinhagen, C. B. Mullins, K. J. Stevenson and B. A. Korgel, *J. Am. Chem. Soc.*, 2011, **133**, 20914-20921.
2. G. Jaksa, B. Stefane and J. Kovac, *Surf. Interface Anal.*, 2013, **45**, 1709-1713.
3. N. Shirahata, T. Yonezawa, W.-S. Seo and K. Koumoto, *Langmuir*, 2004, **20**, 1517-1520.
4. S. Seal, S. Krezoski, D. Petering and T. L. Barr, *Appl. Surf. Sci.*, 2001, **173**, 339-351.
5. T. P. Nguyen and S. Lefrant, *J. Phys.: Condens. Matter*, 1989, **1**, 5197.
6. E. Radvanyi, E. De Vito, W. Porcher and S. Jouanneau Si Larbi, *J. Anal. Atomic Spec.*, 2014, **29**, 1120-1131.
7. B. Philippe, R. Dedryvere, M. Gorgoi, H. Rensmo, D. Gonbeau and K. Edstrom, *Chem. Mater.*, 2013, **25**, 394-404.
8. M. Y. Nie, D. P. Abraham, Y. J. Chen, A. Bose and B. L. Lucht, *J. Phys. Chem. C*, 2013, **117**, 13403-13412.
9. C. Önnby and C. G. Pantano, *J. Vac. Sci. Technol. A*, 1997, **15**, 1597-1602.
10. K. Miyoshi and D. H. Buckley, *Appl. Surf. Sci.*, 1982, **10**, 357-376.
11. G. B. Smith, D. R. McKenzie and P. J. Martin, *Phys. Status Solidi B*, 1989, **152**, 475-480.
12. D. Wheeler and S. Pepper, *Surf. Interface Anal.*, 1987, **10**, 153-162.
13. J. I. Langford and A. J. C. Wilson, *J. Appl. Cryst.*, 1978, **11**, 102-113.
14. P. Scardi, M. Leoni, and R. Delhez, *J. Appl. Cryst.* 2004, **37**, 381-390.